A Theoretical Study of the Crystal $HgCl_2$ Compound

Meng-Sheng Liao[*,#] **and Qian-Er Zhang**

State Key Laboratory for Physical Chemistry of Solid Surfaces, Chemistry Department, Xiamen University, Xiamen 361005, P. R. China

(Received October 5, 1998)

A theoretical study of the crystal $HgCl_2$ compound has been done using a quasi-relativistic density-functional method. The crystalline environment was simulated by a cut-off type Madelung potential. Bond length, dissociation energy, force constants, and sublimation enthalpy are calculated. The calculated properties are in goon agreement with available experimental data. The calculated difference in bond length between the isolated and crystalline molecule is consistent with the data obtained by the more recent gas-phase electron diffraction and X-ray single crystal measurements. The predicted symmetrical and antisymmetrical force constants (k^s, k^{as}) and their trend ($k^{as} > k^s$) are in accordance with the Raman and IR data. The trend is in contrast to the free molecule case, where $k^{as} < k^s$. The sublimation enthalpies of hypothetical HgX_2 (X = F, Cl, Br, I) compounds with the XeF_2-type structure are evaluated. It is shown that the XeF_2-type structures for HgX_2 are significantly less stable than the actual structures.

Among the solid-state mercury(II) halides, $HgCl_2$ is the only compound that has a molecular lattice. HgF_2 crystallizes with the fluorite (CaF_2-type) structure; $HgBr_2$ and HgI_2 have layer lattices. A structural feature of crystalline $HgCl_2$ compound is that $HgCl_2$ 'molecules' are isolated. The distance between an Hg and the Cl from the next $HgCl_2$ is large (3.37 Å), and the nearest Cl atoms are 3.33 Å apart (see Table 2). These separations are comparable to the sums of the van der Waals radii (R_{Hg}^{vdW} = 1.50 Å, R_{Cl}^{vdW} = 1.80 Å).[1] So there are no significant short intermolecular interactions in the structure. It is well established from experience that solid compounds that contain rather localized building blocks can often be well treated by the "embedded cluster approximation". I.e. a group of atoms is treated by a molecular quantum mechanical method, while the environment is simulated in an approximate manner. A number of theoretical approaches to account for the crystal environment have been established for ionic compounds. One of the practical methods is based on the point-charge model, in which the interactions due to other atoms in the crystal are simulated by a potential of point-charges. It was shown that such a model is able to give satisfactory results.[2—5] The solid $HgCl_2$ is a suitable compound for investigation by the point-charge model.

The crystal structure of $HgCl_2$ was previously analyzed by Braekken and Scholten[6] using X-ray powder diffraction. They gave the Hg–Cl bond length of 2.25 Å. Using X-ray single crystal diffraction technique, Subramanian and Seff[7] re-measured the crystal structure and obtained the Hg–Cl bond length of 2.291 Å. The latter value is believed to be likely precise. We note the gas-phase $HgCl_2$ has the Hg–Cl bond length of 2.252 Å, according to the more recent electron diffraction investigation.[8] Therefore the Hg–Cl bond length in the solid state is about 0.04 Å longer than in the gas phase. One of the purposes of this work is to examine if the difference between the gas-phase and solid-state bond lengths could be reproduced by including crystal field effects in the calculation. In earlier electron diffraction studies of gaseous $HgCl_2$, the Hg–Cl bond lengths were measured to be 2.28 Å,[9] 2.34 Å,[10] 2.27 Å,[11] 2.29 Å.[12] So, from the calculated results, we could judge which experimental data are reliable.

Another question is the one of crystal structure type. It is known that all mercury(I) halides Hg_2X_2 have regular tetragonal structures with space group *I4/mmm* (Fig. 1a);[13] they are isotypic with the XeF_2 structure (Fig. 1b).[14] However, none of the mercury(II) halides HgX_2 crystallizes in the XeF_2-type structure. Is there a simple reason for the deformation? Besides, we want to make predictions for some other properties (force constants and vibrational frequencies) of $HgCl_2$ in the crystal structure. These properties have been experimentally measured for the solid-state compound and show different behavior than those of the gas-phase molecule.

Computational Method

The calculations were done using the Amsterdam density-functional (ADF) program developed by Baerends and co-workers.[15] The ADF method uses the expansion of the one-electron molecular orbital in atomic-centered STO basis sets. The specified core electrons are described in the frozen-core approximation.[15a] Many useful exchange-correlation potential functionals are included, such as X_α exchange; VWN's (Vosko, Wilk, and Nusair) correlation;[16] Becke's nonlocal exchange;[17] Perdew's nonlocal correlation.[18] They can be combined to give various functionals. Integrals are computed by the three-dimensional numerical integration method.[15b] Relativistic effects on the electronic structures are evaluated by the quasirelativistic method.[19]

In this work, the simple X_α-potential (α = 0.7) was chosen

Present address: Department of Chemistry, University of Puerto Rico, P.O. Box 23346, San Juan, PR 00931, USA.

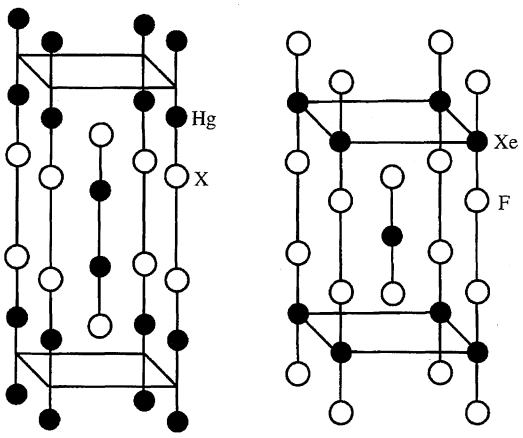

(a) Hg_2X_2 (b) XeF_2

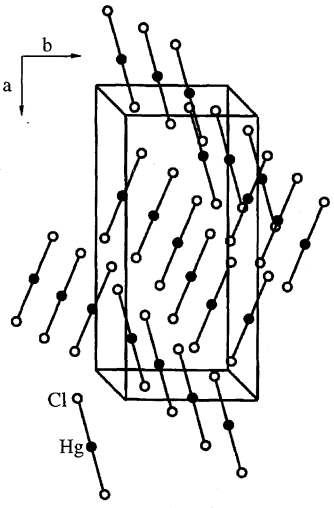

(c) $HgCl_2$

Fig. 1. Unit cells of Hg_2X_2, XeF_2 and $HgCl_2$.

since more sophisticated potentials were shown not to improve the results for this kind of system.[20] The main shortcoming of the DFT is that it is unknown how the functional of the exchange-correlation energy could be improved in a systematic way towards the exact expression. It was claimed that the VWN-B-P functional could give accurate binding energies for both main-group and transition-metal systems.[21] However, the conclusion may not be true for some particular systems. We found that the VWN-B-P functional greatly underestimates the dissociation energy of $HgCl_2$, and also gives too long a bond length (see Table 3).

The STO basis used is of triple-zeta quality. For Hg, the 5d and 6s shells were considered as valence shells; two 6p and one 5f polarization functions were added (ζ_{6p} = 2.60, ζ_{6p} = 1.35, ζ_{5f} = 2.70). For Cl, 3s and 3p were considered as valence shells and one 3d polarization function was added (ζ_{3d} = 1.65). The other shells of lower energy were treated as core and kept frozen.

Crystal Structure and Crystal Field Modeling

The crystal $HgCl_2$ is orthorhombic with space group *Pnma*. A unit cell is shown in Fig. 1c and the lattice constants are given in Table 1. The positional parameters for the crystal and the nearest interatomic distances are given in Table 2. Within a $HgCl_2$ molecule, the Hg–Cl1 and Hg–Cl2 bond lengths are slightly different. The discrete linear Cl–Hg–Cl molecules are arranged in sheets, stacked one above another along the $\vec{c}$ axis. To take into consideration the effects of the crystalline environment, the atoms outside the calculated molecule are replaced with point charges of +2 and −1, attached to the Hg and Cl lattice sites, respectively. The effects of all (infinite) point charges are then summed up to convergence by a Madelung-type treatment.[22] The Madelung potential is first evaluated on a point grid in the spatial region of the molecular group and is then simulated by fitted changes at a finite number of surrounding points of the real crystal lattice. In deciding the positions of the lattice sites, the Hg–Cl1 and Hg–Cl2 distances were set to be equal. So the positional parameters in Table 2 are slightly adjusted. The spatial region is given by the spherical volumes of radius 2.5 Å around the Hg and of radius 2.2 Å around the two Cl's. In this case, 78 point-charges at the (nearest) lattice sites have been used to build up the crystalline environment. The error of the fitted potentials is less than 0.002 eV. Because the simple point-charge model neglects the short-range overlap from the nearest neighbors, a slight modification for the Madelung potential, V_{Madelung}, has been made by using a Coulomb cut-off type pseudopotential

$$V_{\mathrm{eff}}(r) = \mathrm{Max}(V_{\mathrm{Madelung}}(r), C). \quad (1)$$

Here Max means to give the maximum value of the arguments. Equation 1 accounts for the fact that the valence electrons of the ion group must not penetrate into the electrostatically attractive core regions of the surrounding an- or cat-ions because of the Pauli exclusion repulsion. C is a constant used in cut-off type effective core potentials[23] to balance the nuclear attraction.

The bond energy in the crystal field (CF) is defined as: AB

Table 1. Crystal Structure Data[a] and the Used Bond Lengths[a]

Compound	Crystal structure data	Bond length used
$HgCl_2$	Orthorhomic, *Pnma*, $Z=4$, $a=12.765$, $b=5.972$, $c=4.330$	Hg–Cl = 2.291 (exptl)
$HgCl_2$ (hypoth)	Tetragonal, $I4/mmm$, $Z=2$, $a=b=4.48$, $c=8.11$	Hg–Cl = 2.29
HgF_2 (hypoth)	$a=b=3.67$, $c=7.99$	Hg–F = 1.95
$HgBr_2$ (hypoth)	$a=b=4.66$, $c=8.29$	Hg–Br = 2.45
HgI_2 (hypoth)	$a=b=4.92$, $c=8.77$	Hg–I = 2.63

a) Lattice constants and bond lengths are in Å.

Table 2. Positional Parameters[a] for Crystal $HgCl_2$ and the Nearest Interatomic Distances

	x	y	z	Nearest interatomic distances (Å)
Hg	0.1400 (0.1405)[b]	0.25	0.3342 (0.3290)	Hg–Cl = 2.291 (2×),[c] Hg–Cl* = 3.37[d] (2×)
Cl1	0.2810	0.25	0.6581 (0.6580)	Hg–Hg = 4.33 (2×), Cl–Cl = 3.33 (1×)
Cl2	0	0.25	0	

a) Ref. 7. b) Adjusted values to set Hg–Cl1 and Hg–Cl2 distances equal. c) Coordination numbers. d) Second nearest interatomic distance from the neighboring molecules.

Table 3. Calculated Properties[a] of $HgCl_2$: Free Molecule (FM) and the Molecule in the Crystal Field (MCF)

		R_e	D_e	$\frac{1}{2}E_{latt}$	k_e^s	ω_e^s	k^{as}	ω^{as}
FM	VWN-B-P	2.337	4.12		2.09			
	$X\alpha$	2.299	4.80		2.38	339	2.32	388
	Exptl (gas)	2.252±0.005[b]	4.68[c]		2.596[d]	353.3[d]	2.539[d]	402.5[d]
	ECP-CAS[e]	2.32	3.21					
	ECP-CCI[e]	2.31	3.86					
	PP-MP2[f]	2.293	4.51			346		399
MCF	(A)[g]	2.330	5.58	0.09	2.00	311	2.42	396
	(B)[h]	2.328	5.56	0.08	2.03		2.41	
	Exptl (solid)	2.291(9)[i]	5.55[c]		2.05[j]	315[k]	2.31[j]	388[k]

a) Bond length R_e in Å, dissociation energy D_e in eV, symmetrical and antisymmetrical stretching force constants k_e^s and k_e^{as} in $N\,cm^{-1}$, symmetrical and antisymmetrical stretching vibrational frequencies ω_e^s and ω_e^{as} in cm^{-1}; available experimental data are given for comparison. b) Ref. 8. c) Estimated from standard enthalpies of formation. d) Ref. 26. e) Effective core potential calculations by Stromberg et al.[28] (CAS = complete active space; CCI = contracted CI) f) Pseudopotential MP2 calculation by Kaupp and von Schnering.[29] g) The positions of point-charges are not optimized. h) The positions of point-charges have been optimized. i) Ref. 7. j) Evaluated from the experimental frequencies. k) Ref. 30.

(in CF)→A (free) + B (free). It now consists of two parts

$$E_{bond}^{total} = \frac{1}{2}E_{latt} + E_{bond}^{internal}, \quad (2)$$

where $E_{bond}^{internal}$ is the bond energy of the molecule, as calculated in the crystal field. E_{latt} is the electrostatic interaction between the atoms (or fragmentns) and the lattice

$$E_{latt} = \sum_A \left[\int \rho_A(\vec{r}) \cdot V_{eff}(\vec{r}) \cdot d\vec{r} + Z_A \cdot V_{eff}(R_A) \right], \quad (3)$$

where ρ_A is the electronic density of atom A, Z_A the nuclear charge of A, and R_A the position vector of A.

We have been tempted to ask why $HgCl_2$ does not crystallize in the XeF_2-type (i.e. *I4/mmm*) structure. To evaluate the relative stability of an XeF_2-type structure versus the *Pnma* structure, a hypothetical crystal $HgCl_2$ compound with the XeF_2-type structure was calculated. The hypo-$HgCl_2$ is isotypic with Hg_2Cl_2, where an Hg–Hg pair is replaced by a single Hg. So the lattice constant $a(=b)$ and Cl···Cl distance (in the $\vec{c}$ direction) of the hypo-$HgCl_2$ can be assumed to be equal to those of Hg_2Cl_2. On the other hand, the Hg–Cl bond length in the hypo-$HgCl_2$ can be assumed to be equal to that in the real $HgCl_2$. The lattice constant c is calculated as: $c = 2R(Hg–Cl) + R(Cl\cdots Cl)$. In the process of calculations, we have also evaluated the relative stabilities of hypothetical HgF_2, $HgBr_2$, and HgI_2 crystal compounds, which are supposed to have the XeF_2-type structure. The lattice constants of these hypothetical compounds were calculated as was done for $HgCl_2$ except that we used the experimental Hg–X bond length in the gas phase plus 0.04 Å to approximate the Hg–X bond length in the solid state. The obtained lattice constants and Hg–X bond lengths used for various hypothetical halides are given in Table 1. Although there may be some errors in the adopted lattice parameters, calculated results are usually very insensitive to some changes in the positions of point-charges.[20] The presented results will also clarify this point. The qualities of basis sets used for F, Br, and I are triple-zeta plus one polarization.

Results and Discussion

The results (bond lengths, dissociation energies, force constants, vibrational frequencies) of $HgCl_2$, for both free molecule (FM) and molecule in the crystal field (MCF), are presented in Table 3. The dissociation energy is defined as

$$HgCl_2(FM/MCF) \rightarrow Hg(free) + 2Cl(free). \quad (4)$$

There are no direct measurements of dissociation energies for $HgCl_2$. The experimental values given in Table 3 are those estimated from standard enthalpies of formation of the gas-phase and solid-state compounds. The relevant ΔH_f° data are:[24,25] $HgCl_2(g)$, −1.52 eV; $HgCl_2(s)$, −2.39 eV; Hg(g), 0.64 eV; Cl(g), 1.26 eV.

For comparison, the calculated properties of free $HgCl_2$ molecule are also of interest. They give some impression of the accuracy of the applied density-functional method. They are also the reference points for discussing the effects of crystal field on $HgCl_2$. The experimental bond length given in Table 3 is the datum from the more recent gas-phase electron diffraction study.[8] For free $HgCl_2$, two kinds

of the DF approximations were used: the simple X_α and the more sophisticated VWN-B-P potential. Compared with the experimental data, the VWN-B-P potential gives too long a bond length (by ca. 0.1 Å) and too small force constants; the dissociation energy is also notably underestimated (by 0.56 eV). In contrast, the X_α potential gives better results in all the cases (for R, D, k). Therefore we decided to adopt the simple X_α potential for the calculations here. The X_α value of R_e is about 0.05 Å too long. Correspondingly, the calculated force constants (symmetrical and antisymmetrical) are about 0.2 N cm^{-1} smaller than the experimental values.[26] The latter result also indicates that the calculated bound length is indeed somewhat overestimated. The calculated dissociation energy for the free molecule agrees well with the 'experimental' one, the error being 0.1 eV (2%). The calculation shows that the symmetrical force constant k^s is 0.06 N cm^{-1} larger than the antisymmetrical one k^{as}. This is in full agreement with the experimental finding.

There have been some theoretical calculations on the free $HgCl_2$ molecule. Wadt[27] calculated electronic structure of $HgCl_2$ using effective core potential (ECP) in conjunction with a CI wave function; the results were used to assign the absorption spectra and to explain the photo-dissociation. Stromberg et al.[28] also did some ECP calculations on $HgCl_2$. Their CAS and CCI methods give 0.06—0.07 Å too long bond lengths and seriously underestimate the dissociation energy. More recently, Kaupp and von Schnering[29] reported qausi-relativistic pseudopotential (PP) calculations of $HgCl_2$ at the MP2 level. They give a bond length that is very close to our calculated value; the other PP-MP2 data are also quite comparable to the X_α values.

We now put $HgCl_2$ in the crystal field. As the first step, all point-charges are placed at positions set by the X-ray diffraction study and the central molecule is optimized in this crystal field. Because the optimized Hg–Cl bond length may differ from the experimental one, the experimental positions of point-charges are hence not consistent with the calculated bond length. To examine the influence of the change of crystal structure on the calculated properties, the resulting new bond length in the first step is then transferred to all coordinating $HgCl_2$ molecules to correct the field. According to Table 2, the Hg–Cl bond length and the lattice constants have the following relationship

$$\sqrt{(0.1405 \times a)^2 + (0.329 \times c)^2} = R_{HgCl}. \quad (5)$$

We assume that the lattice constant b and the the ratio a/c(= 12.765/4.33 = 2.948) remain unchanged for the respective Hg–Cl bond lengths. In Table 3, the MCF is labeled by (A) and (B) with following meaning: (A) — The positions of point-charges are not optimized; (B) — The positions of point-charges have been optimized. In the case of (A), the calculated bond length is about 0.04 Å (4 pm) longer than the crystalline value. From (A) to (B), the bond length is 0.002 Å (i.e. 0.2 pm) shortened; the other properties (D, k) are also very slightly changed. So the modified crystal field is unimportant in the calculations. The same conclusion was drawn also by other authors.[4] For the hypothetical compounds, the optimized bond lengths in the crystal field are longer than the bond lengths used by 0.01—0.05 Å (see Tables 1 and 4). The deviations are not large, and therefore the calculated properties of the hypothetical HgF_2, $HgBr_2$, and HgI_2 compounds in the un-optimized structures could stand for the actual theoretical results.

The Hg–Cl bond lengthens by 0.03 Å upon going from FM to MCF. The calculated bond length shift is consistent with the experimental finding (0.04 Å). Corresponding to the Hg–Cl bond expansion in the CF, there is a decrease of 0.4 N cm^{-1} in the force constant k^s. A notable feature here is that in the CF, the antisymmetrical force constant k^{as} is shown to be significantly larger than k^s. This is in contrast to the free molecule case. Adams and Appleby[30] have recorded the Raman and IR spectra for the solid-state $HgCl_2$. At 1 bar and 150 K, the symmetric and antisymmetric vibrational frequencies are shown to be 315 cm^{-1} (ν_1) and 388 cm^{-1} (ν_3), respectively. From these data, we may evaluate 'experimental' symmetric and antisymmetric force constants. They are found to be k^s = 2.05 N cm^{-1} and k^{as} = 2.31 N cm^{-1}. The magnitudes and the trend agree with the calculated results. Again, the calculated dissociation energy of MCF is very close to the 'experimental' value estimated from the thermodynamic data. According to the Mulliken population analysis, the molecule becomes more polarized in the solid state (Mulliken atomic charge Q_{Hg} = 1.14 e; Q_{Cl} = −0.57 e) than in the gas phase (Q_{Hg} = 0.90 e, Q_{Cl} = −0.45 e). This is usual.

By comparison of the calculated energies between FM and MCF, we can calculate the sublimation enthalpy of the solid

Table 4. Calculated and Experimental Sublimation Enthalpies (ΔH_{sub})[a)]

	Structure type	ΔH_{sub}^{calc}	ΔH_{sub}^{exptl}	R^{calc} (A)
$HgCl_2$	*Pnma* (real)	18.0	18.5	2.33
	XeF_2-type (hypoth)	11.6		2.33
HgF_2	CaF_2-type (real)		16	
	XeF_2-type (hypoth)	4.6		1.96
$HgBr_2$	$Cmc2_1$ (real)		18.8	
	XeF_2-type (hypoth)	11.3		2.48
HgI_2	$Cmc2_1$ (real)		19.9	
	XeF_2-type (hypoth)	8.9		2.68

a) ΔH_{sub} is in kcal mol^{-1} (1 eV = 23.06 kcal mol^{-1}); experimental data are cited from Ref. 24.

compound, viz. $\Delta H_{sub} = D_e$ (MCF) $- D_e$ (FM). It is shown from Table 4 that experimental ΔH_{sub} is nicely reproduced by the calculation. Because the calculated ΔH_{sub} is the difference between D_e (MCF) and D_e (FM), the possible errors caused by the density-functional used will cancel. This indicates that the crystal field model is capable of describing the effects of the crystalline environment quite accurately. The good agreement of the theoretical and experimental sublimation enthalpies gives us some confidence in the other calculated values. The relative stability of the hypothetical structure versus the real one can be evaluated by comparing their ΔH_{sub} values. So, it is found that for $HgCl_2$ the XeF_2-type structure is 6.4 kcal mol^{-1} (0.28 eV) less stable than the *Pnma* structure. For HgF_2, the XeF_2-type structure has rather small ΔH_{sub}, while the typically ionic CaF_2-type structure has much larger ΔH_{sub}. In the cases of $HgBr_2$ and HgI_2, the XeF_2-type structures are also significantly less stable than the real $Cmc2_1$ structures. So the calculated ΔH_{sub} data clearly disfavor the XeF_2-type structures for all HgX_2 compounds.

Conclusions

We arrive at the following main conclusions from the results:

(i) This point-charge model is quite suitable for the study of the crystal $HgCl_2$ compound. The experimentally measured crystal field effects are well reproduced by the calculations.

(ii) The Hg–Cl bond undergoes an expansion of 0.03 Å on going from the gas phase to the solid state. This result supports the experimental data obtained by the more recent gas-phase electron diffraction[8] and X-ray single crystal[7] measurements. Earlier experimental data[6,9–12] on the bond length are more or less in error.

(iii) The symmetrical and antisymmetrical force constants for the crystal compound are predicted to be 2.0 and 2.4 N cm^{-1}, respectively. The magnitudes and their trend are in agreement with the Raman and IR data on the solid-state compound. However, the gas-phase molecule shows different behavior, where the antisymmetrical force constant is slightly smaller than the symmetrical one.

(iv) The hypothetical HgX_2 compounds with the XeF_2-type structure are all significantly less stable than the actual structures, thus accounting for the fact that none of the HgX_2 compounds prefers the XeF_2-type structure.

We are grateful to the referees for their constructive comments and to Professor Y. Ishikawa for reading the manuscript.

References

1 R. C. Weast et al., "CRC Handbook of Chemistry and Physics," 68th ed, CRC Press, Inc., Boca Raton, Florida (1987).

2 J. Almlöf and U. Wahlgen, *Theoret. Chim. Acta*, **28**, 161 (1973).

3 S. Saebø, B. Klewe, and S. Samdal, *Chem. Phys. Lett.*, **97**, 499 (1983).

4 a) P. Popelier, A. T. H. Lenstra, C. Van Alsenoy, and H. J. Geise, *Acta Chem. Scand.*, **A42**, 539 (1988). b) P. Popelier, A. T. H. Lenstra, C. Van Alsenoy, and H. J. Geise, *J. Am. Chem. Soc.*, **111**, 5658 (1989). c) A. T. H. Lenstra, C. Van Alsenoy, K. Verhulst, and H. J. Geise, *Acta Crystallogr., Sect. B*, **B50**, 96 (1994).

5 a) M.-S. Liao, Q.-E. Zhang, and W. H. E. Schewarz, *Inorg. Chem.*, **34**, 5597 (1995). b) M.-S. Liao and W. H. E. Schewarz, *J. Alloys Compd.*, **246**, 2 (1997). c) M.-S. Liao and Q.-E. Zhang, *Inorg. Chem.*, **36**, 396 (1997).

6 H. Braekken and W. Scholten, *Z. Kristallogr.*, **89**, 448 (1934).

7 V. Subramanian and K. Seff, *Acta Crystallogr., Sect. B*, **B35**, 2132 (1980).

8 K. Kashiwabara, S. Konaka, and M. Kimura, *Bull. Chem. Soc. Jpn.*, **46**, 410 (1973).

9 H. Braune and S. Knoke, *Z. Phys. Chem.*, **B23**, 163 (1932).

10 A. H. Gregg, G. C. Hampson, G. I. Jenkins, P. L. F. Jones, and L. E. Sutton, *Trans. Faraday Soc.*, **33**, 852 (1937).

11 L. R. Maxwell and V. M. Moseley, *Phys. Rev.*, **57**, 21 (1940).

12 P. A. Akishin, V. P. Spiridinov, and A. N. Khodchenkov, *Zhur. Fiz. Khim.*, **33**, 20 (1959).

13 a) E. Dorm, *J. Chem. Soc., Chem. Commun.*, **1971**, 466. b) R. J. Havighurst, *J. Am. Chem. Soc.*, **48**, 2113 (1926).

14 H. A. Levy and P. A. Agron, *J. Am. Chem. Soc.*, **85**, 241 (1963).

15 "ADF Program Package, Version 2.0.1": a) E. J. Baerends, D. E. Ellis, and P. Ros, *Chem. Phys.*, **2**, 41 (1973). b) G. te Velde and E. J. Baerends, *J. Comput. Phys.*, **99**, 84 (1992).

16 S. H. Vosko, L. Wilk, and M. Nusair, *Can. J. Phys.*, **58**, 1200 (1980).

17 A. D. Becke, *Phys. Rev.*, **A38**, 3098 (1988).

18 J. P. Perdew, *Phys. Rev.*, **B33**, 8822 (1986).

19 T. Ziegler, V. Tschinke, E. J. Baerends, J. G. Snijders, and W. Ravenek, *J. Phys. Chem.*, **93**, 3050 (1989).

20 M.-S. Liao, Ph.D. Thesis, Universität Siegen, Shaker, Aachen (1993).

21 a) B. G. Johnson, P. M. W. Gill, and J. A. Pople, *J. Chem. Phys.*, **98**, 5612 (1993). b) J. Li, G. Schreckenbach, and T. Ziegler, *J. Am. Chem. Soc.*, **117**, 486 (1995). c) C. Heinemann, R. H. Hertwig, R. Wesendrup, W. Koch, and H. Schwarz, *J. Am. Chem. Soc.*, **117**, 495 (1995).

22 P. P. Edward, *Ann. Physik*, **64**, 253 (1921).

23 W. Kutzelnigg, R. J. Koch, and W. A. Bingel, *Chem. Phys. Lett.*, **2**, 197 (1968).

24 B. J. Aylett, in "Comprehensive Inorganic Chemistry," ed by J. C. Bailar, H. J. Emelús, and A. Trotman-Dickinson, Pergamon Press, New York (1973), Vol. 3.

25 I. Barkin and O. Knache, "Thermochemical Properties of Inorganic Substances," Springer, Berlin (1973).

26 A. Givan and A. Loewenschuss, *J. Chem. Phys.*, **64**, 196 (1976).

27 W. R. Wadt, *J. Chem. Phys.*, **72**, 2469 (1980).

28 D. Stromberg, O. Gropen, and U. Wahlgren, *Chem. Phys.*, **133**, 207 (1989).

29 M. Kaupp and H. G. von Schnering, *Inorg. Chem.*, **33**, 2555 (1994).

30 D. M. Adams and R. Appleby, *J. Chem. Soc., Dalton. Trans.*, **1977**, 1530.